



# Numerical Modelling of Deformation for Partially Saturated Slopes Subjected to Rainfall

Binod Tiwari, Katsuyuki Kawai, and Phommachanh Viradeth

## Abstract

Rainfall is one among the most common contributing factor and trigger for landslides. In the majority of the cases, slopes are at partially saturated condition when they are subjected to rainfall. While analysing stability of those slopes, deformation analysis is performed in a conservative way assuming the slope to be in a fully saturated condition. In this research, a fully coupled hydro-mechanical finite element model is described based on the constitutive model developed for partially saturated soil condition. A 1.2 m long and 0.6 m high sandy slope was modelled in laboratory and was subjected to 30 mm/h of rainfall for 3 h. Values of suction measured after 3 h were very close to the numerically calculated values based on the finite element method developed by the authors. This model was used to calculate deformation of slope for different intensities of rainfall and at different angles of slopes in order to predict the amount of deformation or failure condition when a slope is subjected to a continuous rainfall of different intensities and durations.

## Keywords

Rainfall • Partially saturated soil • Suction • Deformation • Constitutive model • Cam Clay model • Shallow landslides

## Background

Rainfall is considered as one among the most common contributing factors and triggers of shallow landslides. While evaluating stability of slopes subjected to rainfall, slopes are generally considered to be saturated. Therefore, shear strength of saturated soil is used for analysis. However, in majority of cases, the slopes remain partially saturated during rainfall. Therefore, analysis that is done for the

assumed saturated condition gives conservative results. In this study a 1.2 m × 1.2 m × 0.6 m sized sandy slope is modelled in laboratory and was subjected to a rainfall of 30 mm/h for 3 h. Values of suction were measured with time for the entire 3 h period. The models were prepared with three different angles of inclinations but at the same void ratio of 0.6. A constitutive model that was developed for the partially saturated condition was utilized for the numerical analysis of the slopes.

B. Tiwari (✉)

Fullerton, Civil and Environmental Engineering Department,  
California State University, 800 N State College Blvd., E-419,  
Fullerton, CA 92834, USA  
e-mail: [btiwari@fullerton.edu](mailto:btiwari@fullerton.edu)

K. Kawai • P. Viradeth

Department of Civil Engineering, Kobe University, 1-1 Rokkoudaicho  
Nadaku, Kobe 657-0013, Japan  
e-mail: [kkawai@kobe-u.ac.jp](mailto:kkawai@kobe-u.ac.jp); [pviradeth@gmail.com](mailto:pviradeth@gmail.com)

## Experimental and Numerical Modelling

### Experimental Modelling

In the experimental setup, a sandy soil was compacted in a Plexiglas container at the void ratio of 0.6. The experimental model is presented in Fig. 1. This model is instrumented with four high-precision tensiometers at different locations under

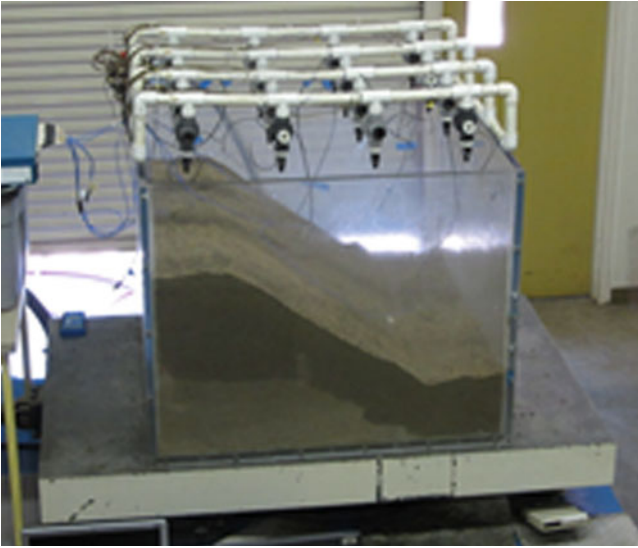


**Fig. 1** Overview of the experimental model—change in color shows the water front

the ground. Values of suction were measured at those locations during rainfall. The suction values were recorded in every 15 min interval. Depths of water front were also recorded from outer sides of the Plexiglas container in every 15 min for the entire rainfall period.

## Numerical Modelling

Critical state shear strength of soil was obtained by conducting CU triaxial test on the saturated sand following ASTM procedure. Likewise, consolidation and swelling parameters of the saturated soil were obtained through one-dimensional consolidation test as per the ASTM standard. Test results were helpful to obtain critical state friction angle and developing p-q curves to obtain the critical state parameters. The geotechnical properties of the saturated sand obtained from the pertinent soil tests are summarized below.

Compression index =  $C_c = 0.2$ ; Swelling index =  $C_s = 0.02$ ;  $M$ : Critical state line = 0.74; Effective Friction Angle =  $31.8^\circ$ ; Effective Cohesion = 0

Deformation analysis of the slope was performed using the modified Cam Clay model based on the approach proposed by Karube and Kawai (2001), which was latter improved by Ohno et al. (2007). Numerous constitutive models for unsaturated soil have been proposed since Bishop (1960) presented the concept of effective stress for unsaturated soils (e.g., Alonso et al. 1990; Karube et al. 1996; 1997). Ohno et al. (2007) developed a relationship between changes in stiffness of unsaturated soil with effective degree of saturation. Kawai et al. (2007) explained the model in

detail. In this model, application of the soil-water retention characteristic curve (SWRCC) model can be used independently in the constitutive model. Kawai et al. (2007, 2009) successfully utilized this model in various geotechnical applications pertinent to unsaturated soils including natural slopes and embankments. According to the proposed model, effective stress is expressed as follows:

$$\boldsymbol{\sigma}' = \boldsymbol{\sigma}^{net} + p_s \mathbf{1} \quad (1)$$

Where,

$$\boldsymbol{\sigma}^{net} = \boldsymbol{\sigma} - p_a \mathbf{1}, \quad p_s = S_e s \quad (2)$$

$$s = p_a - p_w, \quad S_e = \frac{S_r - S_{rc}}{1 - S_{rc}} \quad (3)$$

Here,  $\boldsymbol{\sigma}'$  is effective stress tensor for unsaturated soil,  $\boldsymbol{\sigma}^{net}$  is the net stress tensor,  $\mathbf{1}$  is the second rank unit tensor,  $\boldsymbol{\sigma}$  is total stress tensor,  $s$  is suction,  $p_s$  is suction stress,  $p_a$  is pore-air pressure,  $p_w$  is pore-water pressure,  $S_r$  is degree of saturation,  $S_e$  is effective degree of saturation, and  $S_{rc}$  is degree of saturation at  $s \rightarrow \infty$ . Volume change of soil at certain water content levels is expressed as:

$$e = e_0 - \lambda \ln \frac{p'}{\zeta p'_{sat}} \quad (4)$$

Where,

$$\zeta = \exp[(1 - S_e)^n \ln a] \quad (5)$$

Here,  $a$  and  $n$  are the fitting parameter to express the increase in consolidation yield stress according to de-saturation. Similarly, the plastic volumetric strain is expressed as follows:

$$\varepsilon_v^p = \frac{\lambda - \kappa}{1 + e_0} \ln \frac{p'}{\zeta p'_{sat}} \quad (6)$$

The consolidation yield stress can be obtained as shown in the following equation:

$$p'_c = \zeta p'_{sat} \exp\left(\frac{\varepsilon_v^p}{MD}\right) \quad (7)$$

$$MD = \frac{\lambda - \kappa}{1 + e_0} \quad (8)$$

where,  $p'_c$  is the yield stress represented by mean effective principal stress,  $M$  is  $q/p'$  at the critical state, and  $D$  is the dilatancy coefficient. The following yield function can be obtained by applying the equations presented above in the original Cam Clay model.

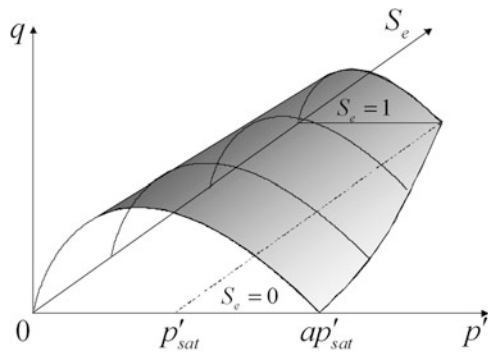


**Fig. 2** Yield surface for unsaturated soil based on the proposed constitutive model

$$f(\boldsymbol{\sigma}', \zeta, \varepsilon_v^p) = MD \ln \frac{p'}{\zeta p'_{sat}} + D \frac{q}{p'} - \varepsilon_v^p = 0 \quad (9)$$

where

$$p' = \frac{1}{3} \boldsymbol{\sigma}' : \mathbf{1}, \quad q = \sqrt{\frac{3}{2}} \mathbf{s} : \mathbf{s}, \quad \mathbf{s} = \boldsymbol{\sigma}' - p' \mathbf{1} = \mathbf{A} : \boldsymbol{\sigma}', \quad \mathbf{A} = \mathbf{I} - \frac{1}{3} \mathbf{1} \otimes \mathbf{1}$$

Here,  $\mathbf{I}$  is the fourth rank unit tensor. Equation (9) reduces to the original Cam Clay model under saturated condition ( $S_e = 1$ ). Figure 2 shows the concept of yield surface expressed by equations presented above.

A Finite Element Modeling (FEM) program was developed for the constitutive model of the unsaturated soil mechanics based on the equations proposed above. The

values of suction calculated from the Finite Element Analysis program explained in earlier chapter were coupled into the FEM setting of the constitutive model for the unsaturated soil mechanics, presented above.

### Results of the Study

Figure 3 presents the values of suction and the velocity of the infiltration within the soil mass after 3 h of rainfall for 30, 45, and 50° slopes. The horizontal and vertical deformation values calculated for slopes with 30, 45 and 50° inclinations after 3 h of rainfall using the FEM analysis are presented in Fig. 4. It shows that the horizontal deformation is maximum near the toe of the slope (Fig. 4). The amount of horizontal deformation is less than 1 mm. The higher the angle of inclination, more the horizontal deformation. The deformation pattern presented in Fig. 4 shows that the slope deformation pattern is more rotational. Likewise, vertical deformation close to 1.5 mm was recorded on top of the slope. The vertical deformation on the ground surface was similar irrespective of the angle of inclination of slopes. Deformations of the slope after the rainfall were measured by redrawing the post-experiment geometry of the slope. Approximately 1.2 mm of settlement was observed on top of the slope and there was less than 1 mm of horizontal deformation. The experimental result was very close to the numerical results presented in Fig. 4.

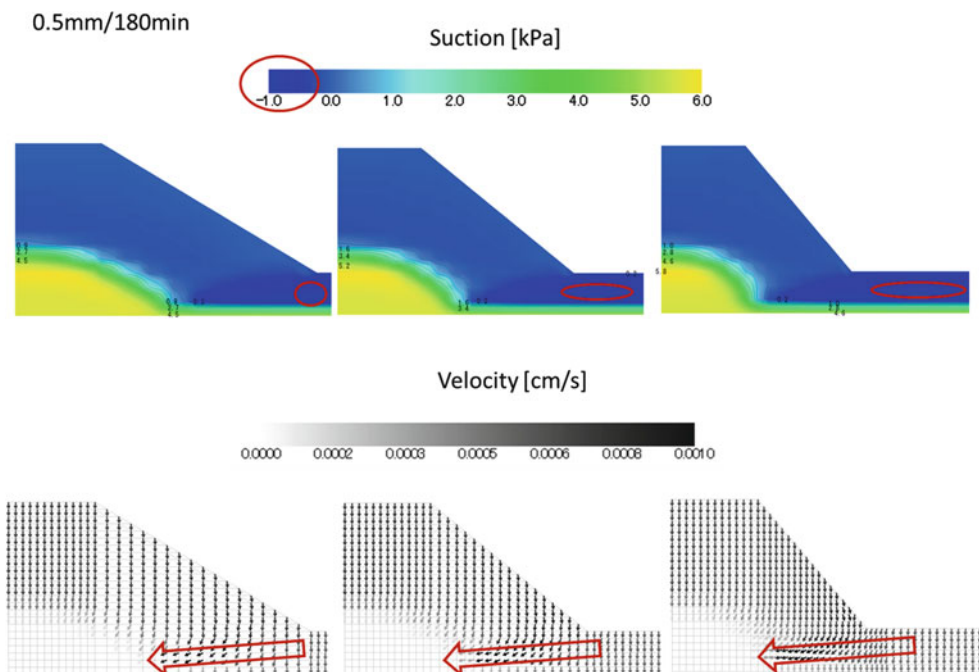


**Fig. 3** Numerically calculated values of suction and the velocity of the movement of water front at various locations of the 30, 45, and 50° slopes after 3 h of rainfall—red circles are the points with positive pore water pressure

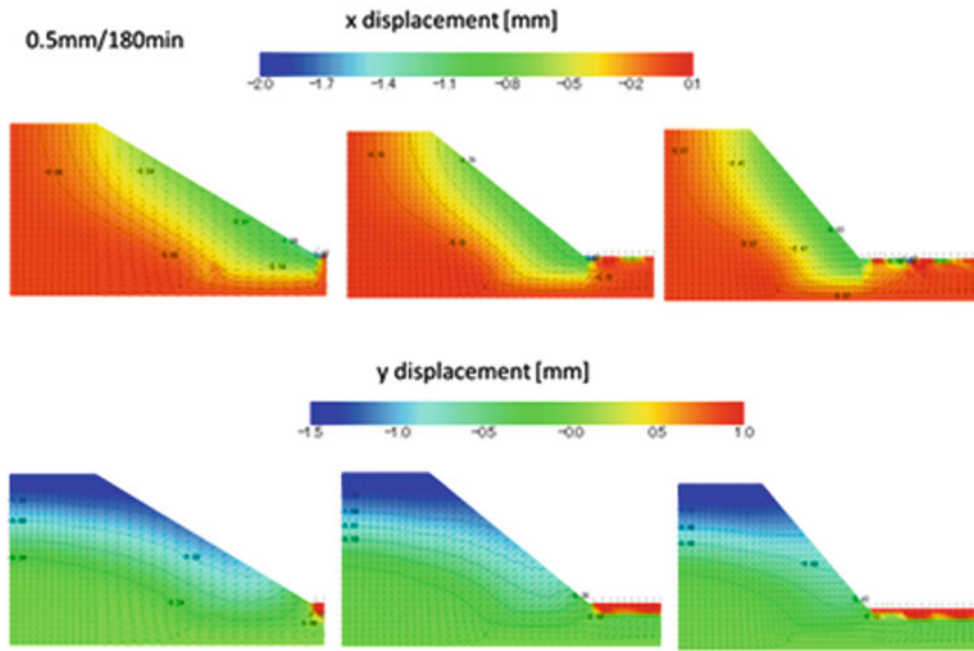


**Fig. 4** Numerically calculated values of deformation at various locations of the 30, 45, and 50° slopes after 3 h of rainfall

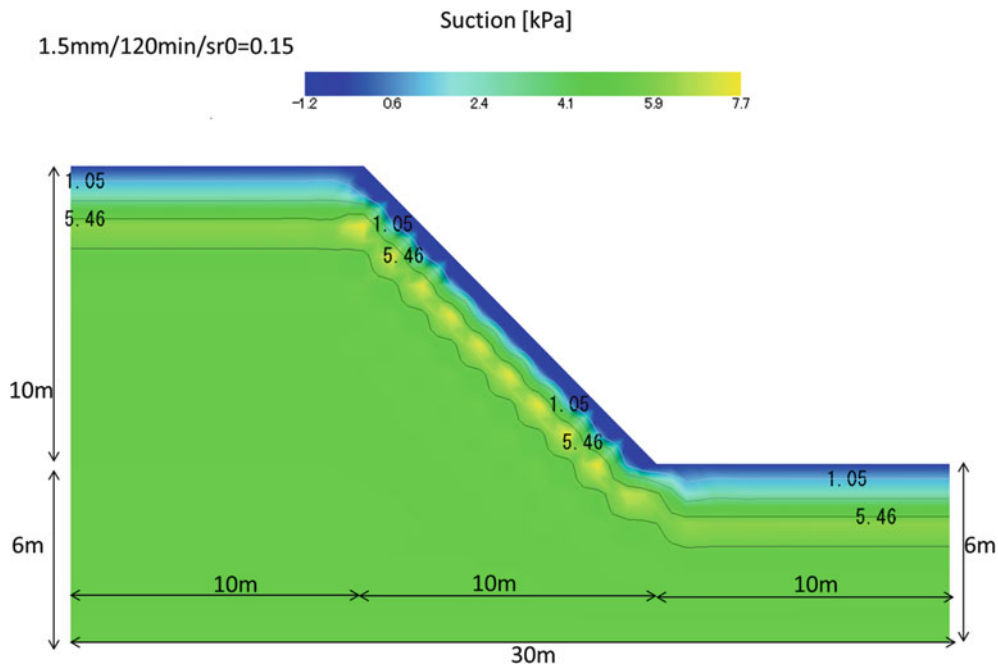


**Fig. 5** Numerically calculated values of suction and movement of water front on a conceptual slope after 2 h of rainfall having intensity of rainfall of 90 mm/h

Seepage velocity was estimated using the depth of water-front with time that was calculated using the equations presented earlier and the results presented in Fig. 3. The seepage velocity and the constitutive model was extended to evaluate the temporal change in suction and deformation on a 10 m high slope presented in Fig. 5. Slope presented in Fig. 5 is a conceptual slope prepared for the purpose of

parametric study only. The geotechnical and hydraulic properties of soil obtained for the experimental model slope was used as the geotechnical properties of the conceptual slope. Presented in Fig. 6 are the values of suction recorded after 2 h of rainfall having intensity of 90 mm/h. The pattern of the numerical values of suction and velocity of water front were similar (or proportional) to the small

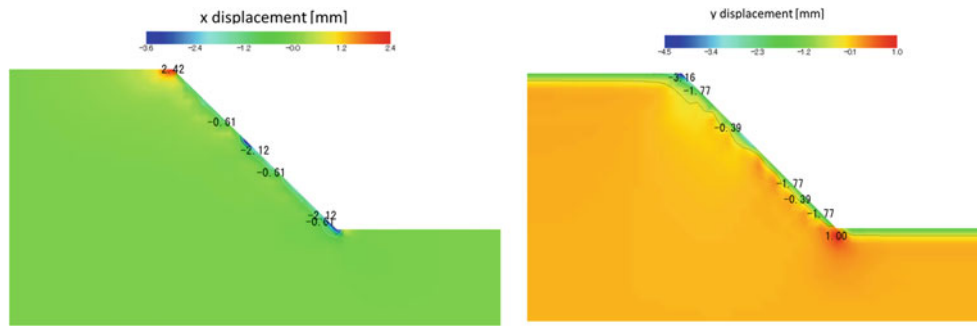


**Fig. 6** Numerically calculated values of deformation on a conceptual slope after 2 h of rainfall having intensity of rainfall of 90 mm/h

scale slope used for the experimental modelling. The deformations of slope in x and y axes (i.e. horizontal and vertical direction) are presented in Fig. 6. As observed in Fig. 6, small outward deformation of less than 3 mm (locally) was observed near the head of the slope. The toe of the slope showed an inward deformation i.e. shrinkage. This shows that unless the rainwater percolated downwards along the slope to touch the toe of the slope, the deformation near the toe is negligible.

#### Summary and Conclusion

In order to study the effect of rainfall on soil-suction and soil deformation, sandy slopes were prepared at three different angles of inclinations. These slopes were subjected to 30 mm/h of rainfall for 3 h, separately, using a rain simulator. The amounts of suction with the duration of rainfall at different locations were measured with tensiometers. A hydro-mechanical model was developed for unsaturated soil condition using the finite element method. Modified Cam Clay model was utilized to prepare the models. The models are capable to couple the unsaturated seepage flow and associate suction into the deformation analysis. The study result shows that the calculated values of suction and deformation were similar to the values observed during the experimental modelling. The numerical analysis for a conceptual 10 m high slope shows that the variations in suction on larger slopes are proportional to the variation in suction in a small scale model. Likewise, the deformation of slope near the toe is negligible if the rainwater is not capable of moving infiltrating to the toe of the slope.

**Acknowledgement** The authors would like to thank the California State University Fullerton for providing sabbatical leave and the Kobe University, Japan for providing visiting professorship for the first author during the period of this collaborative research. We also would like to thank the graduate students from the research laboratory of the second author for running some numerical models pertinent to this study.

#### References

- Alonso EE, Gens A, Josa A (1990) A constitutive model for partially saturated soils. *Geotechnique* 40(3):405–430
- Bishop AW (1960) The principle of effective stress. *Norwegian Geotechnical Institute* 32:1–5
- Karube D, Kawai K (2001) The role of pore water in the mechanical behavior of unsaturated soils. *Geotech Geol Eng* 19(3):211–241
- Karube D, Kato S, Hamada K, Honda M (1996) The relationship between the mechanical behavior and the state of pore water in unsaturated soil. *J Jpn Soc Civil Eng* 535(III-34): 83–92 (in Japanese)
- Karube D, Honda M, Kato S, Tsurugasaki K (1997) The relationship between shearing characteristics and the composition of pore water in unsaturated soil. *J Jpn Soc Civil Eng* 575(III-40): 83–92 (in Japanese)
- Kawai K, Iizuka A, Hayakawa E, Wang W (2007) Non-uniform settlement of compacted earth structures caused by the deformation characteristics of unsaturated soil on wetting. *Soils Found* 47 (2):195–205
- Kawai K, Iizuka A, Tachibana S, Ohno S (2009) Impacts of plant induced uptake on the stability of the earth structure. *Proc International Conference on Soil Mechanics and Geotechnical Engineering*, Alexandria 1:526–529
- Ohno S, Kawai K, Tachibana S (2007) Elasto-plastic constitutive model for unsaturated soil applied effective degree of saturation as a parameter expressing stiffness. *J Jpn Soc Civil Eng* 63 (4):1132–1141